

ChemComm

Accepted Manuscript



This article can be cited before page numbers have been issued, to do this please use: J. Zhang, V. Singh, T. Guo, H. Xu, L. Wu, K. J. Gu, C. Wu and R. Gref, *Chem. Commun.*, 2017, DOI: 10.1039/C7CC03471G.



This is an Accepted Manuscript, which has been through the Royal Society of Chemistry peer review process and has been accepted for publication.

Accepted Manuscripts are published online shortly after acceptance, before technical editing, formatting and proof reading. Using this free service, authors can make their results available to the community, in citable form, before we publish the edited article. We will replace this Accepted Manuscript with the edited and formatted Advance Article as soon as it is available.

You can find more information about Accepted Manuscripts in the [author guidelines](#).

Please note that technical editing may introduce minor changes to the text and/or graphics, which may alter content. The journal's standard [Terms & Conditions](#) and the ethical guidelines, outlined in our [author and reviewer resource centre](#), still apply. In no event shall the Royal Society of Chemistry be held responsible for any errors or omissions in this Accepted Manuscript or any consequences arising from the use of any information it contains.



Journal Name

COMMUNICATION

Moisture resistant and biofriendly CD-MOF nanoparticles obtained via cholesterol shielding

Received 00th January 20xx,
Accepted 00th January 20xxVikramjeet Singh^{a, b}, Tao Guo^a, Haitong Xu^c, Li Wu^a, Jingkai Gu^c, Chuanbin Wu^b, Ruxandra Gref^{d*},
Jiwen Zhang^{a*}

DOI: 10.1039/x0xx00000x

www.rsc.org/

A facile and one step-method was developed to enhance the water stability of CD-MOF nanoparticles through surface modification with cholesterol. CD-MOFs were able to maintain their cubic crystalline structures even after 24 hrs incubation, well tolerated *in vivo* and could increase up to 4 times the blood half-life of DOX.

Metal organic frameworks (MOFs) are a versatile class of porous and crystalline material with potential applications in gas storage and separation, catalysis, sensors and drug delivery.^{1–5} The MOFs gained increased attention in recent years due to their chemical versatility and tunable porosity, but unfortunately, the practical applications are hampered in many cases by their moisture-sensitive nature⁶. For instance, γ -cyclodextrin based MOFs (γ -CD-MOFs) are a class of almost perfectly shaped, crystalline and porous materials build by coordination of γ -CDs and potassium (K) ions^{7,8}. The γ -CD-MOFs have become very popular in reason of their biocompatibility and prospective applications in gas storage and biomedicine^{9,10}. However, these applications face serious challenges related to the poor stability of γ -CD-MOFs which rapidly disintegrate when exposed to the humid conditions. Nevertheless, only three strategies have been reported so far to improve the stability of γ -CD-MOFs in water. Furukawa et al. used ethylene glycol diglycidyl ether to crosslink γ -CD-MOFs to produce γ -CD-MOF hydrogels¹¹. However, the synthesis was time-consuming, taking more than three days at 65 °C and several steps were required to remove the unreacted crosslinker. Recently, Li et al. incorporated fullerene (C60) in the γ -CD-MOF the matrices in an attempt to increase their aqueous stability¹². However, the supramolecular assemblies did not maintain their structure over prolonged times and eventually degraded in water after 24h incubation due to the weak interaction between C60 γ -CDs and in CD-MOFs.

Moreover, the occupancy of γ -CD cavities by C60 might also reduce the capacity of γ -CD-MOFs to load drugs. Very recently, we successfully cross-linked the γ -CD using diphenyl carbonate to get water insoluble cubes¹³. However, the crystalline structure was lost after cross-linking and 8 hrs Soxhlet extraction was required to remove the byproduct phenol. Thus, there is still an urgent need to develop CD-MOFs with good stabilities in aqueous environments, without affecting their porous and crystalline structure nor their ability to incorporate drugs. The elaboration of such water-“shielded” CD-MOFs would pave the way towards their applications in drug delivery and other fields.

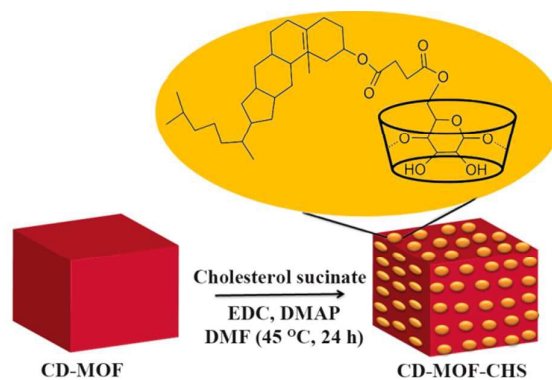


Figure 1. Schematic illustration of CD-MOF surface modification by cholesterol (CHS).

Herein, we developed a straightforward one-step and effective strategy to graft cholesterol (CHS) to form a protective hydrophobic layer over the surface of CD-MOF in order to enhance their aqueous stability (Fig. 1). CHS is one of the most common endogenous physiological molecules that has been tremendously used in self-assembly, nanoparticle modification and hydrophobicity enhancement of various systems^{14–16}. According to recent studies, nanoparticles made from biocompatible polymers and coated with CHS were shown to effectively deliver anti-cancer drugs, nucleic acids used in gene therapy, and imaging agents inside cells, irrespective of the

^a Center for drug delivery system, Shanghai Institute of Materia Medica, 201210, Shanghai (China). Email: jwzhang@simm.ac.cn

^b School of Pharmaceutical Sciences, Sun Yat-Sen University, Guangzhou, China

^c School of Life Sciences, Jilin University, Changchun, 130012, China

^d Institut de Sciences Moléculaires d'Orsay, UMR CNRS 8214 Université Paris-Sud, Université Paris-Saclay 91400 Orsay, France

† Electronic Supplementary Information (ESI) available: [Experimental details, water solvation energy calculations, EDS and pharmacokinetics data. See DOI: 10.1039/x0xx00000x]

COMMUNICATION

shape of the carriers^{17,18}. The CHS shielded CD-MOF (CD-MOF-CHS) developed here turned out to be hydrophobic showing a significant enhancement in water stability and maintained an intact outer and inner crystalline structure.

Nanosized CD-MOFs (~200nm) were synthesized according to our recently published procedure¹⁹. An optimized simple chemical reaction was set up for the surface modification of CD-MOF with CHS using a coupling agent and a catalyst, at 45 °C in DMF for 24 h. The samples were chemically characterized by FTIR and Raman spectroscopies showing a successful linkage of CHS to the hydroxyl groups of γ -CDs in CD-MOFs. For instance, the presence of a carbonyl peak at 1720 cm^{-1} confirmed the conjugated ester linkage in CD-MOF-CHS samples (Figure S-1). As shown in Figure 1A, the specific peak of ester carbonyl in Raman spectra (C=O) at 1668 cm^{-1} can be clearly observed in CD-MOF-CHS, whilst no such signal was obtained in CD-MOF. This again confirmed the successful grafting of CHS to the CD-MOF. The thermal stability of CHS-modified nanoparticles was studied and compared with that of CD-MOF using thermogravimetric analysis and differential scanning calorimetry (Figures S-2 and S-3). It was concluded from these studies that the CD-MOFs contained around 7 wt% grafted γ -CD+CHS.

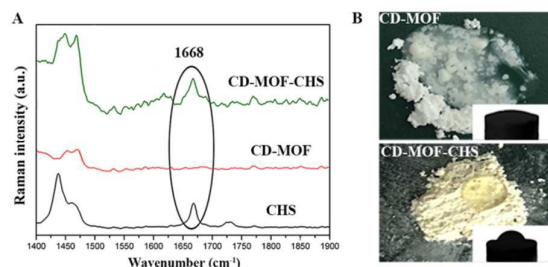


Figure 2. Physicochemical characterizations. Raman spectra of CHS, CD-MOF and CD-MOF-CHS for structural confirmation (A). Digital photographs of CD-MOF and CD-MOF-CHS after placing a drop of water on the nanoparticle powders. Inserts show the water contact angle measurement for the respective samples (B).

The amount of CHS grafted to the CD-MOFs was quantified by high performance liquid chromatography (HPLC). To do so, the CD-CHS covalent bonds were hydrolyzed with ammonia leading to particle disintegration and CHS release. The CHS amount in the CD-MOF-CHS was 3.21 (wt%) which is total agreement of TGA results showing combined 7 (wt%) of γ -CD and CHS (almost doubled due to γ -CD contribution). Supposing that CHS was grafted only to the CDs at the surface of the CD-MOFs, mathematical calculations provided in the supporting information showed that each CD would bear around 5.8 grafted CHS molecules.

Scanning electron microscopy-Energy-dispersive X-ray spectroscopy (EDS) based elemental analysis was used to quantitatively determine the CHS content in the CD-MOF top layers²⁰. The obtained results (Table S-1) showed a sharp decrease in potassium content, from 9.07% (CD-MOF) to 3.39% (CD-MOF-CHS) particles. These findings, together with the increase in carbon and oxygen contents in the CD-MOF-CHS

as compared to the CD-MOF (see SI) clearly indicate the presence of CHS in the top layers of CD-MOF-CHS.

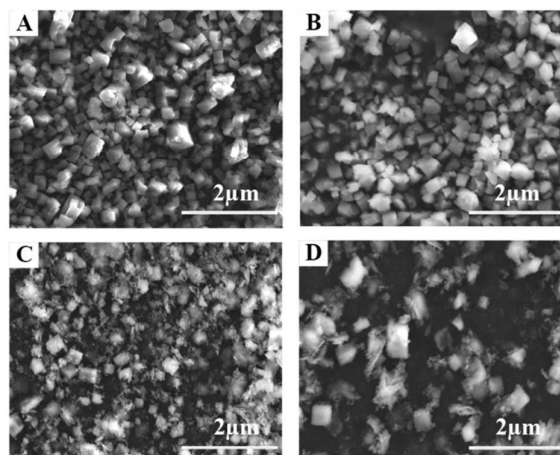


Figure 3. SEM images of CD-MOF (A), CD-MOF-CHS (B), CD-MOF-CHS immersed in water for 12 hrs (C) and 24 hrs (D) in comparison.

The efficacy of the CHS coating on the particle stability in aqueous media was investigated. The instability of CD-MOFs in water is well known. As soon as a water droplet is put on top of a CD-MOF powder, it starts dissolving the particles (Fig. 2B). As a consequence, in water contact angle measurements, the CD-MOF possessed zero water contact angle due to the hydrophilic nature of this material. On the opposite, a drop of water deposited on the top of a CD-MOF-CHS powder adopted a round shape and was not aspired by the powder. A contact angle of 120 ± 1 was recorded, revealing the hydrophobic character of the CD-MOF-CHS (Fig. 2B). Furthermore, the stability in water of the CD-MOF-CHS was tested by immersing the particles in water for 12 and 24 h, respectively. Remarkably it was found that the particles maintained their integrity (Fig. 3), whereas the CD-MOFs control samples immediately disintegrated.

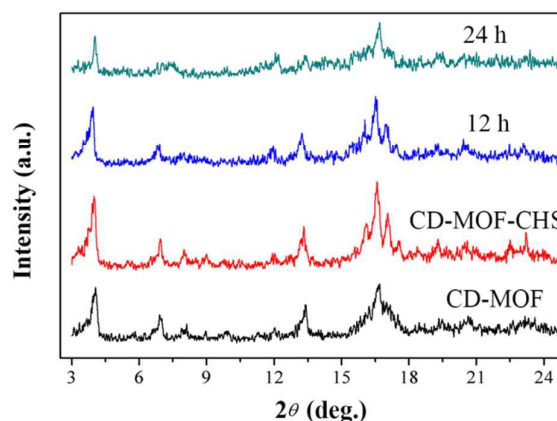


Figure 4. PXRD characterization of CD-MOF and CD-MOF-CHS before and after water treatment for 12 hrs and 24 hrs (C).

The CHS-modified CD-MOFs have similar morphologies and size distributions as their parent CD-MOFs (Fig. 3 A and B), showing that the grafting reaction did not affect their supramolecular structures. After 12 h and 24 h incubation in water the samples retained their cubic shapes, but the edges became rounder (Fig. 3 C and D). These morphological changes could be attributed to water penetration inside the network, leading to progressive degradation. It was therefore interesting to study if CD-MOF-CHS maintained their crystalline structures in water.

Firstly, X-Ray powder diffraction studies (Fig 4) confirmed that the crystalline structure of the CD-MOFs was intact after their modification with CHS (Fig 4). It is worth mentioning that the other surface modification methods reported so far, such as C60-protection and cross-linking, lead to an almost total loss of crystallinity¹¹. In contrast, even after 12 h incubation in water, the CD-MOF-CHS maintained their crystalline structure (Fig 4). In a nutshell, these data clearly show the potential of CHS grafting to preserve the supramolecular structure of the CD-MOF in aqueous media over long enough periods of time to envisage biomedical applications.

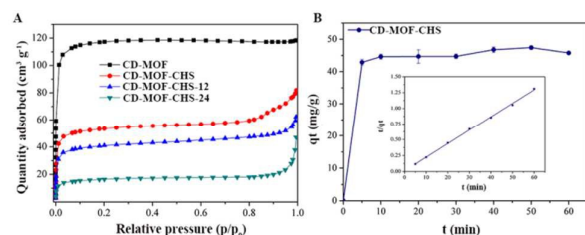


Figure 5.(A) Nitrogen adsorption isotherms for CD-MOF, CD-MOF-CHS and CD-MOF-CHS immersed in water for 12 h and 24 h (B). Time dependent DOX incorporation into CD-MOF-CHS in water. Insert show the linear fit of data using a pseudo-second order kinetic model.

To explain the dramatically increased stability of CHS shielded CD-MOFs in water, simulations were carried on using molecular dynamics to calculate the water solvation energy in CD-MOFs and CD-MOF-CHS samples. The water solvation energy of single CD and single CD grafted with 6 cholesterol molecules were 90.7 kcal/mol and 30.8 kcal/mol, respectively (Figure S-4). The one third decreases in solvation energy after CHS grafting could be one of the main reason of the observed enhanced stability of CD-MOF-CHS particles in water.

The effect of CHS grafting upon the specific surface areas was studied before and after incubation in water (Fig 5). As expected, the surface areas were dramatically reduced upon CHS grafting. Possibly, a dense CHS layer at the particles' surface interfered with N₂ adsorption, leading to an almost 50% reduction of the BET surface areas from 455.1 m²/g to 203.9 m²/g. Of note, the porosity of the CD-MOF-CHS was practically unchanged after immersion in water for 12 h, indicating that degradation was not significant. These data are in agreement with X-Ray diffraction studies (Fig 4) showing a good integrity of the crystalline structures after incubation in water for 12 h. However, further reduction in surface area of

24 h sample was noticed due to progressive degradation as suggested by SEM images.

In conclusion, the CHS-shielded CD-MOF possessed high stability, mesoporous structure, and biofriendly frameworks made of γ -CDs and CHS. These characteristics make CD-MOF-CHS particularly appealing as drug carriers. Herein, we investigated their ability to incorporate DOX, one of the most widely used anticancer drug (see molecular structure in Figure S-5). The CD-MOF-CHS were able to load DOX simply by soaking from aqueous solutions, reaching drug adsorption capacities of 60-80 mg/g (Figure 5B). The DOX absorption was fitted very well with a pseudo-second order kinetic model. The obtained R² value (0.99) suggested that the rate controlling step of adsorptions was mainly the interaction between negatively charged pores and DOX in neutral medium. Moreover, the CD-MOF-CHS particles were able to maintain their crystalline structure after DOX loading as shown in Figure S-6. DOX loaded CD-MOF-CHS showed the feature shift of DOX in ¹H NMR analysis (Figure S-7) which is in complete agreement with previously published study to confirm the DOX presence inside the framework cavities¹². Additionally, elemental analysis was carried out on DOX loaded CD-MOF-CHS cubes using high resolution SEM-EDS device and the presence of nitrogen (attributed to the DOX structure) in high proportion again confirmed the DOX loading (Table S-2).

It is well documented that CHS grafting or modification of DOX-loaded nanoparticles enhances the cellular penetration of DOX²⁰. Similar experiments were carried on here to investigate if the cellular penetration of DOX incorporated in CD-MOF-CHS particles was higher than that of the free drug. HeLa cells stained with DAPI to locate their nuclei were incubated for 4 h with free DOX or DOX-loaded CD-MOF-CHS nanoparticles. Confocal microscopy images showed a higher intensity of DOX signal inside the cells and deposition on cell membranes in the case of DOX-loaded CD-MOF-CHS nanoparticles as compared with free DOX (Fig. 6). Possibly, the CHS shell played a role in promoting cell internalization of the drug as reported previously²¹.

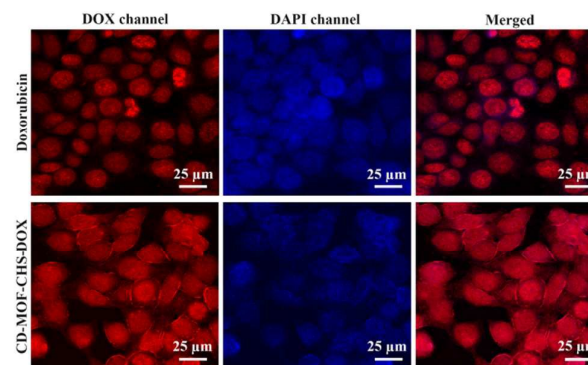


Figure 6. Confocal images of HeLa cells showing cellular uptake of DOX loaded in CD-MOF-CHS at 4 hrs incubation and free DOX in comparison. The nuclei were stained with DAPI (middle). The image was representative of three experiments with similar results.

The CD-MOF-CHS nanoparticles were nontoxic in vitro up to concentrations of 100 μ g/mL as determined by MTT assays (Figure S-8). This encouraged us to test them in vivo. Doses of

5mg/kg of empty CD-MOF-CHS NPs administered by intravenous injection in rats were well tolerated. Finally, DOX-loaded CD-MOF-CHS were administered and their blood clearance was evaluated and compared with free DOX through a pharmacokinetic study.

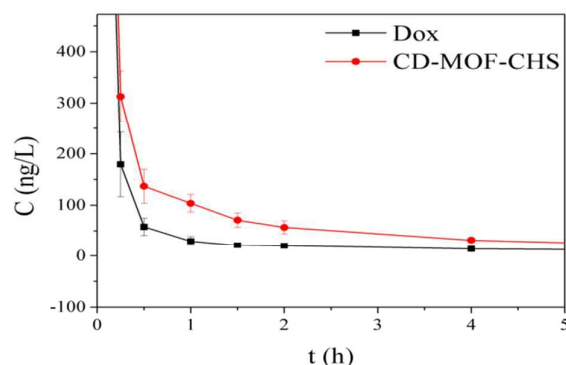


Figure 7. Concentration-time profiles of DOX in plasma of male Sprague-Dawley rats after a single intravenous administration of free DOX and CD-MOF-CHS loaded with DOX (equivalent to 5mg/kg DOX). Experiments were conducted with groups of 8 rats.

As shown in Figure 7, free DOX was rapidly cleared from blood circulation in comparison with the same doses of DOX incorporated in CD-MOF-CHS. This clearly indicates a decrease of DOX clearance from blood. More precisely, the blood circulation half-lives ($t_{1/2}$) of DOX in CD-MOF-CHS were 4 times higher than for free DOX. Moreover, CD-MOF-CHS exhibited significantly increased area under the curve (AUC) in blood, that is, 1.55 times higher than free DOX. All other pharmacokinetic parameters were listed in supplementary table S-3. Possibly the CD-MOF-CHS, stabilized against dissolution in water, allowed a more sustained release of DOX. Further studies will be needed to gain insights on the in vivo fate of CD-MOF-CHS.

In summary, a facile method for the protection of CD-MOF from quick hydration in water via CHS shielding was reported. The coated solids became hydrophobic and were able to retain their porosity, intact morphology and crystallinity even after 24 h of water treatment. The presented methodology to enhance the water stability of CD-MOFs appears more efficient than the previously reported strategy of CD-MOF protection by C60 incorporation. Incorporated DOX was better internalized in cells and in vivo studies showed improved pharmacokinetics of the drug in CD-MOF-CHS as compared to its free form. With further studies, the engineered CD-MOF-CHS nanoparticles, endowed with a biofriendly framework and high drug absorption capacity might find potential applications for drug delivery.

This work was supported by the National Natural Science Foundation of China (81430087).

Notes and references

1. H. Furukawa, K.E. Cordava, M. O'Keeffe, O.M. Yaghi, *Science*, 2013, 341, 1230444.
2. Z. Gou, J. Yu, Y. Cui, Y. Yang, Z. Wang, D.Y. ang, G. Qian, *J. Am. Chem. Soc.*, 2014, 136, 5527.
3. P. Falcaro, R. Ricco, C.M. Doherty, K. Liang, A.J. Hill M.J. Styles, *Chem. Soc. Rev.*, 2014, 43, 5513.
4. J.B. DeCoste, G.W. Peterson, *Chem. Rev.*, 2014, 114, 5695.
5. Zhao, M. Ou S. Wu, C. D. *Acc. Chem. Res.*, 2014, 47, 1199.
6. N.C. Burtch, H. Jasuja K.S. Walton, *Chem. Rev.*, 2014, 114, 10575.
7. R.A. Smaldone, R.S. Forgan, F. Hiroyasu, J.J. Gassensmith, A.M. Slawin, O.M. Yaghi, J.F. Stoddart, *Angew. Chem. Int. Ed.* 2010, 49, 8630-8634.
8. R.S. Forgan, R.A. Smaldone, J.J. Gassensmith, F. Hiroyasu, D.B. Cordes, L. Qiaowei, C.E. Wilmer, Y.Y. Botros, R.Q. Snurr, A.M. Slawin, *J. Am. Chem. Soc.* 2012, 134, 406-417.
9. Gassensmith, J. J. Hiroyasu, F. Smaldone, R. A. Forgan, R. S. Botros, Y. Y. Yaghi, O. M. Stoddart, J. F. *J. Am. Chem. Soc.* 2011, 133, 15312-15315.
10. J.M. Holcroft, K.J. Hartlieb, P.Z. Moghadam, J.G. Bell, G. Barin, D.P. Ferris, E.D. Bloch, M.M. Algaradah, M.S. Nassar, Y.Y. Botros, K.M. Thomas, J.R. Long, R.Q. Snurr, J.F. Stoddart, *J. Am. Chem. Soc.* 2015, 137, 5706-5719.
11. Y. Furukawa, T. Ishiwata, K. Sugikawa, K. Kokado, K. Sada, *Angew. Chem. Int. Ed.* 2012, 51, 10566.
12. H. Li, M.R. Hill, R. Huang, C. Doblin, S. Lim, A.J. Hill, R. Babarao, P. Falcaro, *Chem. Commun.* 2016, 21, 5973.
13. V. Singh, T. Guo, L. Wu, J. Xu, B. Liu, R. Gref, J. Zhang, *RSC Adv.* 2017, 7, 20789-20794.
14. K. Simons, E. Ikonen, *Science*, 2000, 290, 1721-1726.
15. E. Ranucci, M.A. Suardi, R. Annunziata, P. Ferruti, F. Chiellini, C. Bartoli, *Biomacromol.*, 2008, 9, 2693-2704.
16. X. B. Yuan, H. Li, Y. B. Yuan, *Carbo. Poly.*, 2006, 65, 337-345.
17. E. Hinde, K. Thammasiraphop, H. T. Duong, J. Yeow, B. Karagoz, C. Boyer, J.J. Gooding, K. Gaus, *Nat. Nanotechnol.*, 2016, doi: 10.1038/nnano.2016.160.
18. S. Dasgupta, T. Auth, G. Gompper, *Nano Lett.* 2014, 14, 687-693.
19. B. Liu, H. Li, X. Xu, X. Li, N. Lv, V. Singh, J. F. Stoddart, P. York, X. Xu, R. Gref, J. Zhang, *Int. J. Pharma.* 2016, 514, 212-219.
20. D. E. Newbury, N. W. M. Ritchie, *J. Anal. At. Spectrom.* 2013, 28, 973-988.
21. C.J. Chen, J.C. Wang, E.Y. Zhao, L.Y. Gao, Q. Feng, X.Y. Liu, Z.X. Zhao, X.F. Ma, W.J. Hou, L.R. Zhang, W.L. Lu. Q. Zhang, *Biomaterials*, 2013, 34, 5303-5316.